K-shell x-ray-production cross sections in $_6$C, $_8$O, $_9$F, $_{11}$Na, $_{12}$Mg, and $_{13}$Al by 0.75- to 4.5-MeV protons

Y. C. Yu, M. R. McNeir, D. L. Weathers, J. L. Duggan, and F. D. McDaniel
Department of Physics, University of North Texas, Denton, Texas 76203

G. Lapicki
Department of Physics, East Carolina University, Greenville, North Carolina 27858
(Received 10 April 1991; revised manuscript received 8 July 1991)

K-shell x-ray-production cross sections are reported for elements with K-shell x-ray energies between 277 eV (C) and 1487 eV (Al). The x-ray measurements were made with a windowless Si(Li) detector that was calibrated for efficiency by comparing bremsstrahlung spectra from electron bombardment of thin foils of aluminum, silver, and gold with theoretically determined bremsstrahlung spectral distributions. The x-ray-production cross-section measurements are compared to first-order Born and perturbed-stationary-state with energy-loss, Coulomb deflection, and relativistic corrections (ECPSSR) ionization theories using single-hole fluorescence yields. The ECPSSR and first-order Born theoretical predictions are, in general, in close agreement with each other and both generally fit the data quite well.

PACS number(s): 34.50.Fa, 34.70.+e

I. INTRODUCTION

Atomic inner-shell ionization by incident charged particles has been discussed and examined extensively. The literature [1–5] for K-shell x-ray studies with protons indicates a lack of precise data for target atomic numbers less than 13, however. Of the existing K-shell ionization measurements in this region, the earlier measurements used flow-mode proportional counters [6–11]. More precise measurements of cross sections have become possible with the use of high-resolution Si(Li) detectors [12–14]; this is the type of instrument employed in the present study.

There are a number of reasons why the data presented here have not been investigated extensively. First, the Be window of standard Si(Li) detectors, for the most part, attenuates all x rays below 1 keV. Even in the windowless mode the detector efficiency curve is very steep in this region and is difficult to measure. Second, and perhaps of equal importance, is the problem of low-energy contaminant x rays produced by the impurities which are present on the carbon backings used for substrates to support the evaporated targets. These impurities usually come from the soap solution that is used as a surfactant in the preparation of the carbon foils. In this paper, we will outline the techniques that were used to overcome both of these experimental problems.

There have been several theories proposed to explain the measured cross sections. For K-shell ionization of an atom, the direct ionization (DI) of a target electron to the continuum has been shown to be a principal mode of interaction for the region $Z_1 \ll Z_2$ and $v_1 \gg v_{2K}$ (Ref. [15]), where Z_1 and Z_2 refer to the incident and target atomic numbers, and v_1 and v_{2K} refer to the incident-ion and target K-shell electron velocities, respectively. The DI process has been described in the first-order Born approach by the plane-wave Born approximation [15] (PWBA). For $Z_1 \leq Z_2$ and $v_1 \leq v_{2K}$, K-electron capture (EC) to incident-ion bound states is important. The Oppenheimer-Brinkman-Kramers theory as modified by Nikolaev [16] (OBKN) has been used in the first-order Born approach for the EC process. The ECPSSR theory of Brandt and Lapicki for DI [17] and Lapicki and McDaniel for EC [18] accounts for the energy loss (E) and Coulomb deflection (C) of the projectile as well as for the perturbed stationary states (PSS) and the relativistic nature (R) of inner-shell electrons. This theory has extended the region of validity to $Z_1 < Z_2$ and $v_1 < v_{2K}$.

This paper reports x-ray production cross sections for protons in the energy range 0.75–4.5 MeV on thin targets of $_6$C, $_8$O, $_9$F, $_{11}$Na, $_{12}$Mg, and $_{13}$Al. X-ray measurements were made with a Link Analytical windowless Si(Li) x-ray detector [19], which allowed the extension of x-ray analysis down to carbon. The ranges of the Z_1/Z_2 and v_1/v_{2K} parameters investigated were $0.076 < Z_1/Z_2 < 0.167$ and $0.43 < v_1/v_{2K} < 2.35$, respectively. The experimental results are compared to the predictions of the first-order Born approximation (PWBA for DI and OBKN for EC) and the ECPSSR theory.

II. EXPERIMENTAL PROCEDURE

Experiments were performed using the 3-MV tandem accelerator (NEC 9 SDH) at the University of North Texas Ion Beam Modification and Analysis Laboratory [20]. Thin targets (see Table I) were prepared by vacuum evaporation and deposition of the elements of interest onto 5-μg/cm^2 carbon foils, except for magnesium, which was evaporated onto gold backings. The impurities on the carbon backings were mainly oxygen, sodium, and silicon. These elements were removed by floating the carbon off in ultrapure water that was spiked with acetic acid [21,22]. The cleaning procedure was repeated three times in an ultrasonic bath. This technique essentially el-

TABLE I. Target specifications.

Element	Substance	Thickness (μg/cm^2)
$_6$C	C	12.3
$_8$O	GeO_2	5.8
$_9$F	LiF	19.2
$_{11}$Na	NaCl	11.4
$_{12}$Mg	Mg	4.6
$_{13}$Al	Al	1.7

iminated the problem of impurity-element x rays.

The Link Analytical windowless Si(Li) detector [19] used for these measurements had an x-ray energy resolution of 135 eV at 5.9 keV. This detector was calibrated for efficiency by comparing atomic-field bremsstrahlung spectra from 66.5-keV electron bombardment of thin foils of aluminum, silver, and gold with the theoretical bremsstrahlung spectral distributions [23,24]. A collimated electron beam from a 300-kV Cockcroft-Walton accelerator was used to produce bremsstrahlung in targets mounted at a 45° angle to the incident beam direction. To prevent scattered electrons from entering the detector, permanent magnets were mounted adjacent to the flight path between the detector and target chambers. The entire apparatus was also carefully shielded from light.

In the experimental scattering chamber, the x-ray detector was mounted at 135° to the incident ion beam direction. A 25-mm^2 silicon surface barrier detector was also mounted at 135° to the incident beam direction to count ions backscattered from the target. The particle detector solid angle was determined with a calibrated radioactive source to be 7.0×10^{-4} sr. Two slit pairs, each with a 1-mm^2 aperture, were used to collimate the incident beam. All of the measurements presented in this paper were made in an ultrahigh vacuum chamber that was maintained at 10^{-8} Torr. The details of this multipurpose chamber have been described elsewhere [20]. The x-ray count rates were kept below 1000 cps in order to avoid excessive pulse pileup. The x-ray pulses were handled by a Link Analytical 2040 System pulse processor [19]. The pulse processor was designed to reduce low-level electronic noise that interfered with low-energy x-ray signals and to provide pulse pileup rejection.

The areas of the x-ray peaks (see Fig. 1) were evaluated using the GUPIX program developed by Maxwell, Campbell, and Teasdale [25]. This program used a digital filter to eliminate background, and then employed a nonlinear Marquardt least-squares-fitting procedure to give a complete analysis of each K-shell spectrum.

III. RESULTS AND DISCUSSION

The K-shell x-ray-production cross section is determined by

$$\sigma_x=\frac{Y_x T_x}{\epsilon N_0 N_1},$$

where Y_x is the number of x rays counted, T_x is a dead time correction for the x-ray detector, and ϵ is the x-ray-detector efficiency for the K x rays; N_0 is the number of protons incident on the target and N_1 is the target thickness in atoms/cm^2.

There is always the question of whether the Rutherford cross section is appropriate for measuring the target thickness. Possible deviations from the Rutherford cross section could have entered from two sources: resonant nuclear scattering and screening effects due to the surrounding electrons. The Coulomb barrier in MeV between the ion and target nucleus was calculated using the formula [26]

$$E_c=1.44Z_1Z_2/R,$$

where Z_1 and Z_2 are the atomic numbers of the two nuclei and

$$R=1.16(A_1^{1/3}+A_2^{1/3}+2.07)$$

is the internuclear separation in femtometers. A_1 and A_2 are the mass numbers of the two nuclei involved in the collision. In the worst case, protons scattered from carbon, the Coulomb barrier was 1.51 MeV in the laboratory reference frame. It has been shown that protons scattering from light target nuclei exhibit non-Rutherford behavior at incident energies above 1 MeV [27–30]. The target thicknesses for this work were measured at a proton energy of 0.75 MeV to overcome this problem. The resulting thicknesses have a total uncertainty of 6% due to uncertainties in solid angle (4%), ion energy (3%), and counting statistics (3%).

The total uncertainty in the measured x-ray-production cross sections was dominated by the uncertainty in the x-ray-detector efficiency, which range from 12% for x-ray energies above 600 eV to 20% for carbon and oxygen x rays. The statistical uncertainty was less

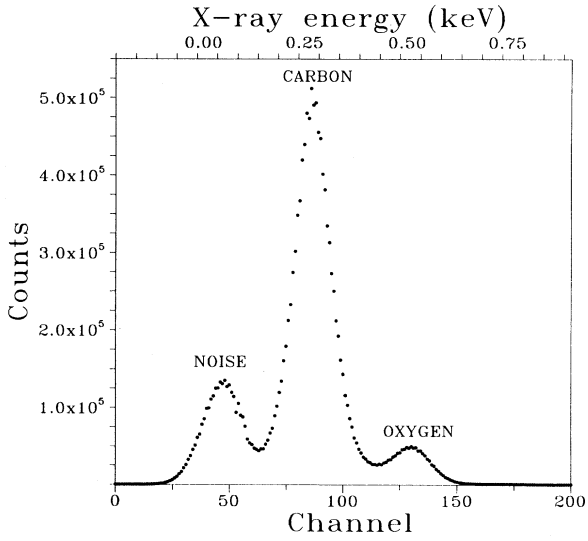

FIG. 1. Typical carbon x-ray spectrum. In the low channels from 25 to 75, a pulse-processor-induced noise peak is seen.

TABLE II. X-ray-production cross sections (in kilobarns) by H^+ ions.

Energy (MeV)		$_6$C	$_8$O	$_9$F	$_{11}$Na	$_{12}$Mg	$_{13}$Al
0.75	Measured	2.72	2.40	1.80	1.01	0.718	0.433
	ECPSSR	2.78	2.13	1.77	0.905	0.643	0.466
	First-order Born	2.68	2.08	1.75	0.921	0.673	0.502
1.0	Measured	2.51	2.66	2.05	1.34	0.962	0.544
	ECPSSR	2.58	2.25	1.99	1.15	0.865	0.663
	First-order Born	2.46	2.17	1.93	1.13	0.870	0.679
1.5	Measured	1.93	2.81	2.21	1.67	1.04	0.849
	ECPSSR	2.20	2.20	2.10	1.39	1.14	0.931
	First-order Born	2.09	2.10	2.01	1.35	1.11	0.919
2.0	Measured	1.74	2.50	2.17	1.77	1.21	1.00
	ECPSSR	1.89	2.05	2.04	1.48	1.26	1.08
	First-order Born	1.80	1.96	1.95	1.43	1.22	1.05
2.5	Measured	1.44	2.27	2.10	1.78	1.32	1.08
	ECPSSR	1.66	1.89	1.94	1.49	1.31	1.15
	First-order Born	1.60	1.81	1.85	1.44	1.26	1.12
3.0	Measured	1.30	2.18	1.98	1.75	1.32	1.19
	ECPSSR	1.48	1.75	1.82	1.47	1.31	1.19
	First-order Born	1.43	1.68	1.75	1.41	1.27	1.15
3.5	Measured	1.29	2.04	1.81	1.72	1.50	1.20
	ECPSSR	1.35	1.62	1.71	1.42	1.30	1.19
	First-order Born	1.30	1.56	1.65	1.37	1.25	1.15
4.0	Measured	1.08	1.92	1.73	1.64	1.43	1.20
	ECPSSR	1.23	1.51	1.61	1.37	1.27	1.18
	First-order Born	1.19	1.45	1.55	1.33	1.23	1.15
4.5	Measured	0.954	1.73	1.64	1.58	1.44	1.20
	ECPSSR	1.13	1.41	1.52	1.32	1.23	1.17
	First-order Born	1.10	1.37	1.47	1.28	1.20	1.13

than 1% for the x-ray yields. The uncertainty from the fitting program was estimated to be less than 3%. This gives an overall uncertainty of 12–15 % for the heavier elements measured and 25% for carbon and oxygen.

The results of our measurements are given in Table II, along with the ECPSSR and first-order Born theoretical predictions. In order to make this comparison, the theoretical ionization cross sections were converted to x-ray-production cross sections by using the single-hole fluorescence yields and transition rates of Krause [31]. The electron-capture contribution to all electronic shells is small, ranging from less than 1% for $_{13}$Al to less than 4% in $_6$C according to the ECPSSR theory. The first-order Born theory predicts an electron-capture contribution of less than 3% in $_{13}$Al to 11% in $_6$C. Figure 2 presents the *K*-shell x-ray-production cross sections as a function of ion beam energy for all of the targets studied in this report. Both the first-order Born (PWBA + OBKN) [15,16] and the ECPSSR [17,18] predictions are shown as well. In addition to the present work, data from other investigations [6–14] are also shown.

For $_6$C, our measurements are shown in Fig. 2 along with measurements by Khan, Potter, and Worley [6], Bissinger, Joyce, and Kugel [10], and Burch [9]. The data of Khan, Potter, and Worley [6] and Bissinger, Joyce, and Kugel [10] are in agreement with our measurements, but the data of Burch [9] are slightly (20–30 %) higher than our data. For oxygen, both of the theories underpredict the data by approximately 15–30 %. For $_9$F, the experimental results of Lennard and Phillips [12] and Kawatsura *et al.* [13] are presented; our results agree quite well with the data of Kawatsura *et al.* in the ion energy range between 1 and 2 MeV, but their data fall below the present results at lower energy. The data of Lennard and Phillips are considerably below our measured values at and below 1 MeV. For $_{11}$Na, the data lie systematically above the predictions of both theories, although with the discrepancy between theory and experiment ranging merely from 10% to 25%. For $_{12}$Mg, the measurements are in good agreement with both theories at ion energies less than 3.0 MeV. The theories seem to slightly underpredict measurements taken above 3.0 MeV. The $_{12}$Mg data of Khan, Potter, and Worley [6] agree with our 1.5-MeV measurement, but they lie well below (30%) our measurements at 0.75 and 1.0 MeV. The $_{13}$Al measurements agree quite well with both theories. The earlier measurement of Basbas, Brandt, and Laubert [8] fall 35% below our data. The measure-

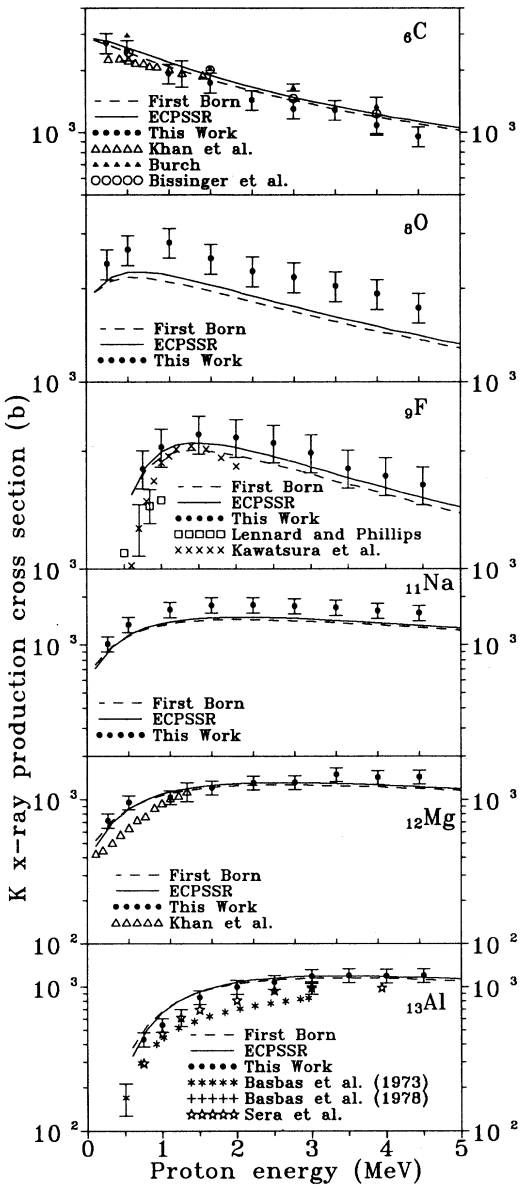

FIG. 2. K-shell x-ray-production cross sections for H^+ ions incident upon carbon, oxygen, fluorine, sodium, magnesium, and aluminum as a function of proton energy. Data are compared to the first-order Born approximation (PWBA plus OBKN) and the ECPSSR theory. The other data are from Refs. [6–14].

ments of Sera *et al.* [14], along with the later measurements of Basbas, Brandt, and Laubert [11] are 15–30% below our data.

IV. CONCLUSIONS

The K-shell x-ray-production cross sections in $_6$C, $_8$O, $_9$F, $_{11}$Na, $_{12}$Mg, and $_{13}$Al have been measured to 0.75–4.5-MeV H^+ ions and are compared to the ECPSSR and first-order Born theories. The first-order Born and ECPSSR theories are in close agreement with each other and the data in the $0.43 < v_1/v_{2K} < 2.35$ range

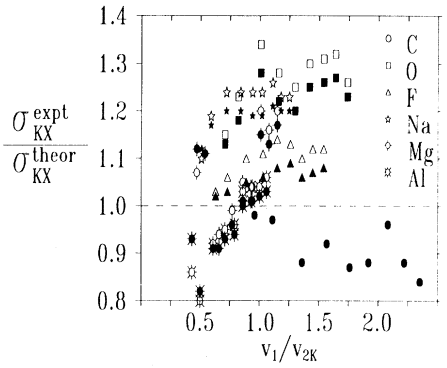

FIG. 3. Ratio of experimental K-shell x-ray-production cross sections (Table I) to theoretical predictions according to the first-order Born (open symbols; Refs. [17] and [18]) vs the proton velocity relative to the electron velocity in the K-shell orbit or the target atom.

of our experiments. Figure 3 illustrates these findings, which are consistent with Figs. 5 and 6 of Ref. [4]. An approximately 10% overestimate of the observed K-shell x-ray production in carbon was also evident in a comprehensive comparison of available data to the predictions of the ECPSSR theory. Furthermore, for v_1 of our data on F, Na, Mg, and Al, both theories—within experimental uncertainties—overlap each other and only slightly underestimate the data. This is consistent with the findings of Ref. [4]. An approximately 25% underestimate of our oxygen data is surprising given that $Z_1/Z_2=0.125$ for this system, which is between $Z_1/Z_2=0.167$ for the carbon data which are overestimated and our remaining data with $Z_1/Z_2 \leq 0.111$ which are only marginally underestimated. We cannot compare this anomalous trend with Ref. [4] since there are no other oxygen data at the relatively high velocities of our experiment where the projectile velocity is of the order of the K-shell electron velocity.

Figure 4 shows a plot of the ratio of experimental K-shell x-ray-production cross sections to the ECPSSR theory versus the target atomic number. Since the aver-

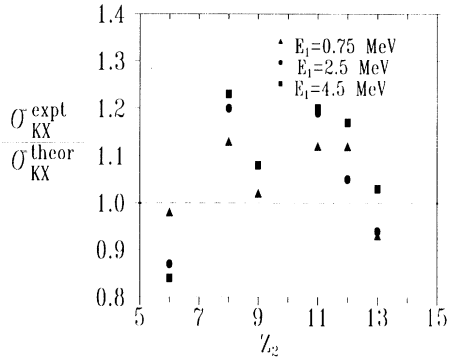

FIG. 4. Ratio of experimental K-shell x-ray-production cross sections to the ECPSSR theory (Refs. [17] and [18]) vs the target atomic number.

age experimental error is ±20% for a typical data point, no conclusive trend can be determined from the figure. In general both theories accurately predict the data and appear to agree better for higher Z_2 (i.e., smaller Z_1/Z_2 system). However, the fluorescence yields and transition rates used did not take into account the effect of multiple ionization of the target atom, which could raise the theoretical predictions for x-ray production above all data points, especially at lowest v_1/v_{2K} where the L shell is more likely to be ionized.

ACKNOWLEDGMENTS

This work was supported in part by the National Science Foundation Grants No. DMR-8812331, INT-8917946, and ECD-9003099, and the Office of Naval Research Grants No. N00014-89-J-1309, N00014-89-J-1344, N00014-90-J-1691, and N00014-91-J-1785, Texas Instruments Inc., Texas Utilities Electric Inc., International Digital Modeling Corp., North Texas Research Institute, Combustion Engineering Inc., Westinghouse Electric Corp., Fluor-Daniels Inc., LTV Corporation, the State of Texas Higher Education Coordinating Board—Texas Advanced Technology Research Program, the Robert A. Welch Foundation, and the University of North Texas Organized Research Fund. The authors would like to thank Dr. R. B. Escue for developing the procedures for producing ultraclean foils, without which the experiment would not have been possible.

[1] H. Paul, Nucl. Instrum. Methods **192**, 11 (1982).
[2] H. Paul, and W. Obermann, Nucl. Instrum. Methods **214**, 15 (1983).
[3] H. Paul, and J. Muhr, Phys. Rep. **135**, 47 (1986).
[4] G. Lapicki, J. Phys. Chem. Ref. Data **18**, 111 (1989).
[5] D. D. Cohen, Nucl. Instrum. Methods B **49**, 1 (1990).
[6] J. M. Khan, D. L. Potter, and R. D. Worley, Phys. Rev. **139A**, 1735 (1965).
[7] G. Bissinger and H. W. Kugel, in *Proceedings of the Interational Conference on Inner Shell Ionization Phenomena, Atlanta, 1972,* edited by R. W. Fink, S. T. Manson, M. Palms, and P. V. Rao (U. S. Atomic Energy Commission, Oak Ridge, TN, 1973), p. 993.
[8] G. Basbas, W. Brandt, and R. Laubert, Phys. Rev. A **7**, 983 (1973).
[9] D. Burch, Phys. Rev. A **12**, 2225 (1975).
[10] G. Bissinger, J. M. Joyce, and H. W. Kugel, Phys. Rev. A **14**, 1375 (1976).
[11] G. Basbas, W. Brandt, and R. Laubert, Phys. Rev. A **17**, 1655 (1978).
[12] W. N. Lennard and D. Phillips, Nucl. Instrum. Methods **166**, 521 (1979).
[13] K. Kawatsura, A. Ootuka, K. Ozawa, F. Fujimoto, K. Komaki, and M. Teresawa, Nucl. Instrum. Methods **170**, 265 (1980).
[14] K. Sera, K. Ishii, M. Kamiya, A. Kuwako, and S. Morita, Phys. Rev. A **21**, 1412 (1980).
[15] E. Merzbacher and H. Lewis, in *Handbuch der Physik,* edited by S. Flugge (Springer-Verlag, Berlin, 1958), Vol. 34, p. 166; G. S. Khandelwal, B. H. Choi, and E. Merzbacker, At. Data **1**, 103 (1969); R. Rice, G. Basbas, and F. D. McDaniel, At. Data Nucl. Data Tables **20**, 503 (1977).
[16] J. R. Oppenheimer, Phys. Rev. **31**, 349 (1928).; H. C. Brinkman and H. A. Kramers, Proc. Acad. Sci. (Amsterdam) **33**, 973 (1930); V. S. Nikolaev, Zh. Eksp. Teor. Fiz. **51**, 1263 (1969) [Sov. Phys.—JETP **24**, 847 (1967)].
[17] W. Brandt and G. Lapicki, Phys. Rev. A **23**, 1717 (1981) for DI.
[18] G. Lapicki and F. D. McDaniel, Phys. Rev. A **22**, 1896 (1980); **23**, 975(E) (1981) for EC.
[19] Link Analytical Ltd., Halifax Rd. High Wycombe, Bucks HP123SE, England.
[20] J. L. Duggan, F. D. McDaniel, S. Matteson, D. E. Golden, J. M. Anthony, B. Gnade, and J. A. Keenan, Nucl. Instrum. Methods B **40/41**, 709 (1989).
[21] P. M. Kocur, J. L. Duggan, R. Mehta, J. Robins, and F. D. McDaniel, IEEE Trans. Nucl. Sci. **NS-30**, 1580 (1983).
[22] D. L. Weathers, J. L. Duggan, R. B. Escue, and F. D. McDaniel, Nucl. Instrum. Methods A **303**, 69 (1991).
[23] D. L. Weathers, J. L. Duggan, M. R. McNeir, Y. C. Yu, F. D. McDaniel, C. A. Quarles, H. Lehtihet, and D. Kahler, Nucl. Instrum. Methods B **56/57**, 964 (1991).
[24] L. Kissel, C. A. Quarles, and R. H. Pratt, At. Data Nucl. Data Tables **28**, 381 (1983).
[25] J. A. Maxwell, J. L. Cambell, and W. J. Teesdale, Nucl. Instrum. Methods B **43**, 218 (1989).
[26] F. K. McGowan (private communications).
[27] M.. Luomajärvi, E. Rauhala, and M. Hautala, Nucl. Instrum. Methods B **9**, 255 (1985).
[28] E. Rauhala, Nucl. Instrum. Methods B **12**, 447 (1985).
[29] J. M. Knox and J. F. Harmon, Nucl. Instrum. Methods B **24/25**, 688 (1987).
[30] E. Rauhala, Nucl. Instrum. Methods B **40/41**, 790 (1989).
[31] M. O. Krause, J. Phys. Chem. Ref. Data **8**, 307 (1979).